

## Two-photon photoelectron spectroscopy of GaP(110) after sputtering, annealing, and multishot laser damage

A. Okano

*Department of Physics, Nagoya University, Furocho, Chikusaku, Nagoya 464-01, Japan*

R. K. R. Thoma, G. P. Williams, and R. T. Williams

*Department of Physics, Wake Forest University, Winston-Salem, North Carolina 27109*

(Received 17 March 1995; revised manuscript received 2 August 1995)

Two-photon photoelectron spectra of GaP have been measured using 3-ps laser pulses of a photon energy below the valence-band photoelectron threshold. Clean,  $1\times 1$  ordered GaP(110) surfaces and surfaces disordered by  $\text{Ar}^+$  sputtering are compared. Delayed excitation/probe measurements set an upper limit of 3 ps on the relaxation time of transiently populated states. Changes in the photoemission spectra have been observed following pulsed-laser irradiation of surfaces with photon energies less than the band gap, and fluences below the threshold of single-shot damage. The changes in the spectrum are discussed with reference to previous studies of laser-induced desorption and damage on GaP.

### I. INTRODUCTION

It is well established that in the high laser fluence regime, ablation is induced by a thermal process, namely, evaporation subsequent to melting.<sup>1</sup> However, it is known that desorption of constituent atoms is induced even at lower fluences without melting from surfaces of some nonmetallic solids. Examples include some compound semiconductors<sup>2,3</sup> and  $\text{Al}_2\text{O}_3$ .<sup>4</sup> Therefore, it has been suggested that electronic processes play an important role in initial stages of laser ablation<sup>3-5</sup> and certain processes of surface modification.<sup>6-9</sup> The fact that laser ablation occurs for irradiation by photons of subband-gap energies on surfaces of wide-gap materials such as  $\text{Al}_2\text{O}_3$  (Ref. 4) and MgO (Refs. 10 and 11) and is initiated most readily from defective surfaces<sup>11</sup> may support this suggestion. For subband-gap photon energies where heating due to band-to-band transitions can be excluded, the primary process of laser ablation is considered to be initiated from defect excitation.<sup>5,11,12</sup>

It has been reported that desorption is initiated from defects on surfaces when a laser pulse of subband-gap energy impinges on clean GaP(110) (Refs. 13 and 14) and GaAs(110) (Ref. 15) surfaces. Hattori and co-workers<sup>13,14</sup> distinguished several stages of laser-induced surface defect processes leading up to ablation. At fluences above  $\approx 0.07 \text{ J/cm}^2$  in a 30 ns pulse for 600 nm light on GaP(110), very weakly bonded atoms proposed to be adatoms on the plane surface were desorbed, gradually decreasing as their number was depleted. With relevance for the present study, we note that  $\text{Ar}^+$  sputtering was shown to greatly increase the number of such weakly bonded atoms desorbed. Above a second desorption threshold  $F_D$  ( $\approx 1.2 \text{ J/cm}^2$  for 600 nm light on GaP), the desorption begins to increase with successive shots. This was suggested to arise from desorption of atoms

bounding vacancies and especially from the boundaries of vacancy clusters, which represent step edges that grow in length as the clusters expand under successive shots. At a still higher fluence of  $F_{ss} \approx 3 \text{ J/cm}^2$ , single-shot ablation yielding a crater visible under an optical microscope takes place.<sup>16</sup> The fluence range between  $F_D$  and  $F_{ss}$  may be regarded as the approach to defect-initiated ablation, in which the number of step-edge defects is increased by the laser light, but breakdown and plasma heating does not occur until after an incubation exposure to many shots. It is, therefore, important to investigate various near-surface phenomena taking place between  $F_D$  and  $F_{ss}$  to understand further the initiation of laser ablation by subband-gap photons.

Among the various excited-state probes that have special sensitivity to the surface of semiconductors, the method of two-photon photoelectron spectroscopy is promising for the ablation initiation regime. This technique offers ultrafast time resolution of excited-state occupancy, excellent sensitivity to surface defect states in the gap,<sup>17</sup> and a very small probed spot, which may be conveniently positioned relative to other laser beams used for desorption and ablation studies. Excited-state properties have been investigated for several Si surfaces using this technique,<sup>17,18</sup> as well as GaAs (Refs. 19 and 20) and InP.<sup>21</sup>

The purpose of this paper is to report properties of excited states and laser-modified defect levels on GaP(110) surfaces observed by two-photon photoelectron spectroscopy. We measured the energy distributions of photoelectrons from transiently populated states excited by 4.66-eV photons on a clean,  $1\times 1$  ordered surface and on a disordered surface prepared by  $\text{Ar}^+$  sputtering. Upper limits on the lifetimes of transiently populated states were measured with 3-ps time resolution. We monitored the effect of surface modification in the fluence regime approaching laser ablation, as registered in the two-photon

photoelectron spectra. For these experiments,  $\text{Ar}^+$  sputtered surfaces were used to enhance the observability of defect-related effects in the surface modification experiments.

## II. EXPERIMENT

The experimental setup has been described in detail elsewhere.<sup>17</sup> We used a mode-locked Nd:YAG (yttrium aluminum garnet) oscillator emitting a continuous train of pulses at 82 MHz. After passing through a fiber/grating pulse compressor, the 1.06  $\mu\text{m}$  pulses were frequency doubled in potassium titanyl phosphate and redoubled in potassium dihydrogen phosphate providing 3-ps pulses of 2.33-eV and 4.66-eV light, respectively. Only 4.66-eV light was used in the measurement of energy distribution spectra of photoelectrons. Both wavelengths were used cooperatively in time-resolved measurements, so that 2.33-eV light populated empty states above the Fermi level, and then 4.66-eV light probed the excited states after a preset delay.

The 4.66-eV beam was focused on the sample surface by maximizing counts in the two-photon spectrum as a function of lens-sample distance, to accurately place the beam waist ( $\sim 10 \mu\text{m}$  diam.) on the sample surface. In this focus condition, the peak intensity of each 3-ps, 4.66-eV pulse was  $\sim 21 \text{ MW/cm}^2$  without attenuation. The average intensity in the focused pulse train was  $\sim 5 \text{ kW/cm}^2$ . However, as shown in Ref. 17, for Si under similar conditions, the peak and average temperature rises are only a few degrees. This is primarily due to rapid conduction into the interior, which remains an excellent heat sink, because of the small spot and consequent small total thermal load ( $\sim 4 \text{ mW}$ ). Photoelectrons were detected by a double-pass cylindrical mirror analyzer (CMA), the resolution of which is about 0.1 eV at the pass-band used.

An *n*-type GaP crystal was polished mechanically and etched chemically in a solution of  $\text{HNO}_3:\text{HCl}:\text{H}_2\text{O}$  (2:1:1) at 55–60 °C to get a (110) mirrorlike surface. The donor concentration was about  $6 \times 10^{17} \text{ cm}^{-3}$ . A clean surface was produced by argon ion sputtering at 1 keV and subsequent annealing at about 600 °C for several minutes in an ultra high vacuum (UHV) preparation chamber. The base pressure of this chamber was  $8 \times 10^{-10}$  Torr. Sharp ( $1 \times 1$ ) low energy electron diffraction (LEED) spots were observed for sputtered and annealed surfaces. On the other hand, no structure was observed by LEED on the  $\text{Ar}^+$  sputtered surfaces. After these procedures, the sample was moved to the main UHV chamber for photoelectron spectroscopy. The base pressure was  $3 \times 10^{-10}$  Torr throughout the measurements.

We used an excimer-pumped dye laser operating at 580 nm (2.14 eV) with 20-ns pulse width to study laser-induced modification on the  $\text{Ar}^+$  sputtered surface. The photon energy is 0.12 eV smaller than the 2.26-eV bulk band-gap energy of GaP at 297 K. The beam size was measured using a knife edge at the focal position of the 4.66-eV light with a quartz lens identical to the one inside the experimental chamber. The 580-nm light on the sample surface had a beam diameter of 170  $\mu\text{m}$  between  $e^{-1}$  points. The dye-laser fluence used for the investiga-

tion was varied between 0.01  $\text{J/cm}^2$  and 1.5  $\text{J/cm}^2$ .  $F_D$  is reported to be 1.0–1.3  $\text{J/cm}^2$  for 580-nm, 30-ns laser pulses.<sup>5,22</sup>

## III. RESULTS AND DISCUSSION

### A. $1 \times 1$ ordered surface

A photoemission spectrum excited by 4.66-eV light of an intensity producing two-photon transitions is shown in Fig. 1 for a clean  $1 \times 1$  ordered GaP(110) surface. The photoelectron counts acquired in 5 s are plotted as a function of the intermediate-state energy  $E_i$  measured relative to the Fermi level  $E_F$ . The photoelectrons whose intermediate states are below  $E_F$  exhibit approximately a linear dependence on intensity, and those with intermediate states above  $E_F$  arise from a two-photon process, exhibiting a quadratic dependence of yield on an intensity well above  $E_F$ . The transition region near  $E_F$  will be discussed later.

The scale of final-state photoelectron kinetic energy  $E_k$ , the directly measured electron energy, is given at the top of Fig. 1.  $E_k$  is related to  $E_i$  as

$$E_k = E_i + h\nu + eV_b - \phi_d,$$

where  $V_b$  is the magnitude of negative sample bias voltage

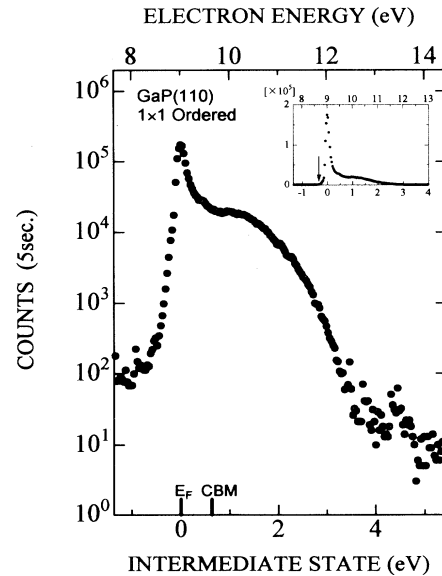


FIG. 1. Photoelectron spectrum for an  $\text{Ar}^+$  sputtered and annealed GaP(110) surface excited by 3-ps pulses of 4.66 eV light at  $21 \text{ MW/cm}^2$ . The energy scale at the top is measured electron kinetic energy, including the  $-8.87\text{-V}$  sample bias. The energy scale at the bottom is the two-photon intermediate-state relative to the Fermi level at the surface. Electron counts per 5-s interval are plotted on a logarithmic scale in the main frame and on a linear scale in the inset. The threshold of the electron counts is indicated by an arrow in the inset.

chosen to improve CMA transmission efficiency and  $\phi_d$  is the work function of the CMA.  $eV_b$  was 8.87 eV for all data and  $\phi_d$  was 4.52 eV. The zero of  $E_i$  is at the Fermi level.

The position of the Fermi level relative to the valence-band maximum (VBM) under strong illumination can be estimated using the value of the valence photoemission threshold of a cleaved GaP(110) surface, which has been measured as 6.01 eV (Ref. 23) or 5.95 eV.<sup>24</sup> Vacuum energy is estimated from the threshold of the spectrum on a linear plot shown in the inset of Fig. 1. The threshold, marked by an arrow, is at  $E_i = -0.34$  eV ( $E_k=8.67$  eV). The work function of this surface, corresponding to  $h\nu + E_i$  at threshold, is therefore deduced as 4.32 eV. Using 5.95 eV as the valence-band photoemission threshold of GaP,<sup>24</sup> the Fermi level position relative to the VBM is thus found to be 1.63 eV for this sample.

It has been reported that the Fermi level position of a sputtered and annealed surface of *n*-type GaP(110) is 1.1 eV (Ref. 25) or 1.2 eV (Ref. 26) above the VBM in the dark or in low illumination condition. In an *n*-type sample at equilibrium, the bands bend upward, because the Fermi level is pinned by surface defect levels<sup>24</sup> in the midgap region [Fig. 2(a)]. Under strong average illumination ( $I_{\text{avg}} \approx 10^{22}$  photons/s cm<sup>2</sup> in this experiment), the bands become flatter so that the VBM at the surface lies farther below the bulk  $E_F$  than in the dark. Based on our finding that the VBM is 1.63 eV below  $E_F$  for strong illumination, the surface photovoltage is apparently about  $-0.5$  eV. The energy distribution curve shown in Fig. 1 has a peak at the Fermi level ( $E_i=0$  eV). This peak is interpreted as originating from surface defects remaining after Ar<sup>+</sup> sputtering and subsequent annealing. It appears that states originating from the surface defects distribute widely in the gap (Fig. 2): a high density of defect states at the middle of the gap is responsible for the Fermi level pinning at low illumination condition<sup>25,26</sup> and we hypothesize that those located higher in the gap are responsible for the peak of the emission yield detected under a high illumination condition in the two-photon photoemission spectrum in Fig. 1. Because of the nonequilibrium nature of the strongly illuminated surface, we hypothesize that defect gap states at least up to the bulk Fermi level are partially occupied, as shown by the schematic shaded density of states in Fig. 2(b). The laser power dependence of photoyield changes sharply from approximately quadratic for  $E_i \geq 0.25$  eV to somewhat sublinear (due to initial state depletion) for  $E_i \leq 0.25$  eV. (The analyzer pass band is about 0.1 eV.) Another reason for sharpness of the observed peak may be the enhancement of photoyield from localized states at threshold, which is well known in atomic physics and was recently observed for surface defect photoemission on Si(111)  $2 \times 1$ .<sup>27</sup> Intrinsic surface states, discussed later, do not appear responsible for the peak at  $E_i = 0$ .

The plateau of the yield from 1 to 2 eV shown in Fig. 1 probably originates from bulk band structure properties. According to the bulk band structure of GaP,<sup>28</sup> a sequence of two direct transitions of  $\approx 4.66$  eV each are possible near the *K* point ( $\langle 110 \rangle$  directed) from the valence

band to an intermediate state in the conduction band and from that conduction state to a final state above the vacuum level. The best match to the photon energies occurs along  $\Sigma$ , about 20% of the way *K* to  $\Gamma$ , at which point the intermediate state is  $\approx 1$  eV above the conduction-band maximum (CBM). The sample orientation was such that the CMA collected electrons about  $10^\circ$  off the normal to the (110) surface. This occurrence of three states separated by 4.66 eV transitions in the bulk band structure may be responsible for most of the plateau of two-photon emission yield between 1 and 2 eV.

The transiently populated intermediate states are, in general, expected to be observed at energies between the Fermi level ( $E_i = 0$ ) and the upper limit  $E_F + 4.66$  eV in Fig. 1. For example, emission from intermediate states all the way to the  $E_F + 4.66$  eV limit is observed on Si.<sup>17</sup> The emission yield from GaP, however, was observed to disappear for  $E_i$  more than 3.9 eV above the Fermi level. The calculated density of states in the conduction-band structure decreases for energies between 4.9 and 5.5 eV

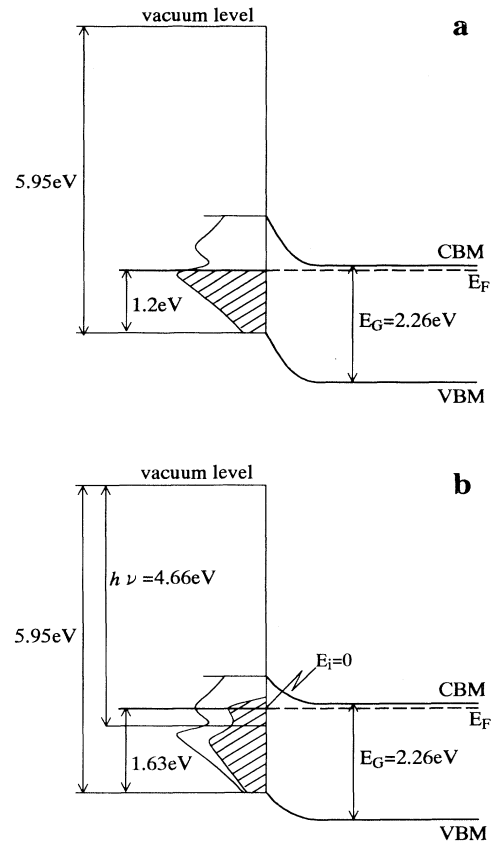


FIG. 2. Suggested schematic distribution of defect states in the gap to account both for photovoltage effects and the observed peak of intermediate states at  $E_i=0$  (i.e., bulk  $E_F$ ) on sputtered/annealed GaP(110). The shaded areas represent electron population at (a) low illumination condition and at (b) high illumination, nonequilibrium condition used in this work.

above the VBM,<sup>28</sup> i.e., 3.13 eV and 3.73 eV relative to the Fermi level on this surface, respectively. This feature of the band structure may account for the gradual decrease of the photoelectron yield in that energy range. Furthermore, as noted above, the good match of sequential 4.66-eV transitions is not found as readily in that intermediate-state range.

According to recent photoemission<sup>29</sup> and inverse photoemission<sup>30–32</sup> studies, the location of the intrinsic unoccupied surface state at the  $\bar{\Gamma}$  point on the GaP(110) surface is assigned at various energies from 0.3 eV below<sup>31</sup> to 0.74 eV above<sup>32</sup> the CBM. The location 0.14 eV above the CBM was favored in Ref. 30, because it is plausible that the intrinsic unoccupied surface state is removed from the gap, and it is located very close to the CBM on GaP(110),<sup>29</sup> as well as other III-V semiconductors such as GaAs(110) (Refs. 33 and 34) and InP(110).<sup>35–37</sup> However, if taken as 0.14 eV above the CBM, the intrinsic unoccupied surface state corresponds to a minimum of the photoelectron yield in Fig. 1. The first reason for the intrinsic unoccupied surface state's not being seen as an important intermediate level in this experiment may be that the 4.66-eV photon does not match a transition between the occupied and unoccupied surface bands, and that bulk conduction electrons may not communicate effectively with the surface on the 3-ps time scale. A second reason is suggested by observations<sup>18</sup> on photoexcited surface states on cleaved Si(111). They observed in that case that emission in-

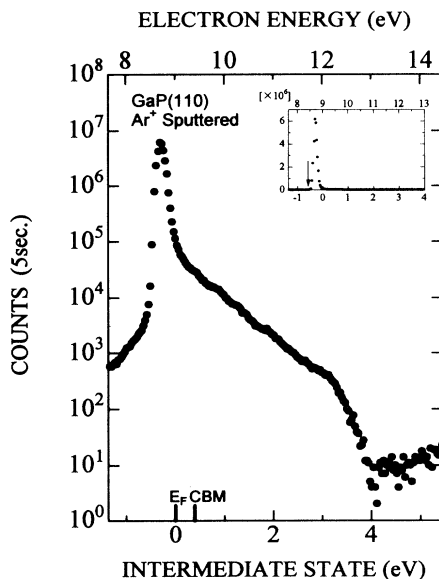


FIG. 3. Photoelectron spectrum for an  $\text{Ar}^+$ -sputtered GaP(110) surface excited by 3-ps pulses of 4.66-eV light at  $21 \text{ MW/cm}^2$ . The energy scale at the top is measured electron kinetic energy, including the  $-8.87\text{-V}$  sample bias. The energy scale at the bottom is the two-photon intermediate state relative to the Fermi level at the surface. Electron counts per 5-s interval are plotted on a logarithmic scale in the main frame and on a linear scale in the inset. The threshold of the electron counts is indicated by an arrow in the inset.

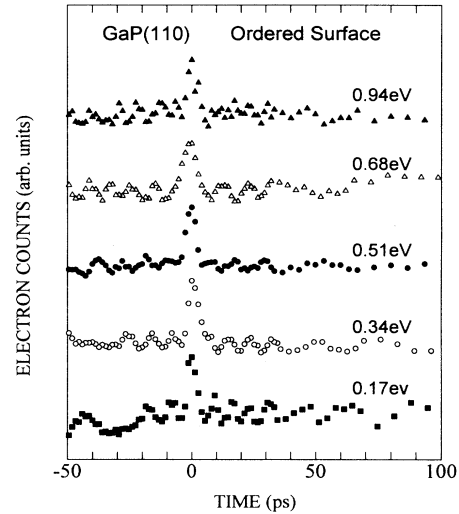


FIG. 4. Time-resolved two-photon photoemission plotted as a function of delay of the 4.66 eV probe pulse relative to the 2.33 eV excitation pulse. The curves are labeled by the intermediate-state energy relative to the Fermi level. Pulse duration was  $\sim 3$  ps.

tensity from the normally unoccupied surface state ( $\pi^*$  state) depends on quality of cleavage and that additional emission, due to cleavage defects such as steps and vacancies appears between the VBM and the peak of the  $\pi^*$  state on a surface of lesser quality. Sputtered and annealed GaP(110) surfaces are confirmed by reflection electron microscopy to be lesser in quality than UHV cleaved surfaces.<sup>38</sup> We hypothesize that the two-photon photoelectron yield from the normally unoccupied intrinsic surface state in this case is too small to be well resolved from extrinsic defect states. Nevertheless, the ratio of the emission yield around the CBM, where the intrinsic unoccupied state is considered to be located, to that in the gap, namely, the ratio of perfect surface lattice sites to defect sites, is much larger for the sputtered and annealed surface than for a disordered surface prepared by  $\text{Ar}^+$  sputtering only. The latter spectrum, shown in Fig. 3, will be discussed in the next section.

Figure 4 shows a result of measurements of the relaxation lifetime of transiently populated states on a  $1 \times 1$  ordered surface. The lifetimes are effectively below our 3-ps resolution limit regardless of the energy of the intermediate states. This is in contrast to measurements on Si by this same technique, for example.<sup>17</sup> Even when it is only 0.17 eV above the Fermi level of GaP, the lifetime of the intermediate state is not longer than the 3-ps pulse width. This suggests that there is a very fast decay channel of scattering and/or surface recombination throughout the midgap region.

### B. $\text{Ar}^+$ -sputtered surface

A typical photoemission spectrum for an  $\text{Ar}^+$ -sputtered surface is shown in Fig. 3. The position of

the Fermi level of the  $\text{Ar}^+$ -sputtered surface is 1.87 eV above the VBM, based on the estimation of the threshold of the yield in the linear plot shown in the inset of Fig. 3.  $E_F$  is located 0.24 eV higher in the gap than for the ordered surface shown in Fig. 1. Straub *et al.*<sup>25</sup> reported insensitivity of the Fermi level position to moderate surface disordering by  $\text{Ar}^+$  sputtering, which still left a partially visible LEED pattern. We used a heavier  $\text{Ar}^+$ -sputtering dose, which obliterated the LEED pattern, so that a shift may be understandable. In particular, since our measurements are for bands only partially flattened by illumination, any treatment that significantly alters the distribution of gap states should cause an apparent shift of the bulk  $E_F$  relative to the band edges.

There is a big linear photoemission peak at  $-0.27$  eV on the scale of intermediate states. We hypothesize that this peak originates from defect states created by  $\text{Ar}^+$  sputtering. As mentioned in the previous section, the larger ratio of the yield at this peak to that around the CBM may indicate an increase of the defect densities and, therefore, the decrease of the intrinsic surface state density on the  $\text{Ar}^+$ -sputtered surface.

Picosecond time-resolved measurements on the  $\text{Ar}^+$ -sputtered surface gave very short lifetimes for several intermediate states from 0.17 to 1.53 eV, just as on the ordered surface indicated in Fig. 4. It is considered that defect sites play a role as surface recombination centers. On both surfaces, the decay time of transiently populated states is shorter than our 3-ps resolution in direct time measurements. The shape of the photoelectron spectrum from the  $\text{Ar}^+$ -sputtered surface in Fig. 3, namely, the lower counts in the high-energy plateau, suggests more rapid relaxation of the higher intermediate states, compared to the ordered surface in Fig. 1.

### C. Multishot laser damage

Figure 5 shows changes of the energy distribution curve following repeated laser irradiation by 20-ns pulses at 580 nm on an  $\text{Ar}^+$ -sputtered surface. The maximum laser fluence was estimated to be  $1.2 \text{ J/cm}^2$ . After the series of 100 pulsed irradiations and measurements represented in Fig. 5, visible damage was observed, but there was no ablation plume. The laser fluence of  $1.2 \text{ J/cm}^2$  is considered to be between  $F_D$  and the single-shot ablation threshold.

The  $170\text{-}\mu\text{m}$  diameter damage spot after 100 shots was observed by scanning electron microscopy and atomic force microscopy. The damage was primarily a fracture, with indications of melting along the fracture edges. Since 580-nm light is below the band gap of GaP, and the laser damage was only observed after multiple shots, the melting indicates defect-induced absorption of the laser light as discussed for subband-gap light on  $\text{MgO}$ .<sup>10,11</sup> Because of the small size of the pulsed laser spot ( $170 \mu\text{m}$ ) relative to the LEED beam, we could not determine if the laser-irradiated surface was ordered. Results reported by Hattori *et al.*<sup>14</sup> for similar laser wavelength and fluence suggest that an ordered surface be-

comes less ordered with repeated shots of  $1.2 \text{ J/cm}^2$ . As the number of laser shots increases, the photoelectron yield from the state at  $-0.27$  eV decreases and a peak at the Fermi level grows. We hypothesize that the sputter-induced defects at  $-0.27$  eV are being replaced by laser-induced surface defects of a different kind. According to the model of Okano *et al.*,<sup>39</sup> pulsed laser irradiation in the fluence range above  $F_D$  should not only remove adatoms, but also produce vacancy cluster defects on the surface and enlarge existing vacancy clusters. One result is the increase of step-edge defects bounding the enlarged vacancy clusters. These may be associated with the laser-induced peak at  $E_F$ . Another possibility for states at  $E_F$  on both sputtered/annealed and laser-irradiated surfaces is the growth of metallic Ga droplets. Long *et al.*<sup>8</sup> have suggested that Ga islands are formed due to laser-induced photochemical decomposition well below the damage threshold fluence on a GaAs(110) surface. At lower fluence, after 1600 shots of repeated irradiation at  $0.84 \text{ J/cm}^2$ , we do not observe growth of the peak at the Fermi level. The surface damage evidently evolves rapidly above a certain threshold laser fluence as measured by Hattori *et al.*<sup>14</sup> through desorption yield.

Another changing feature observed in the spectra of

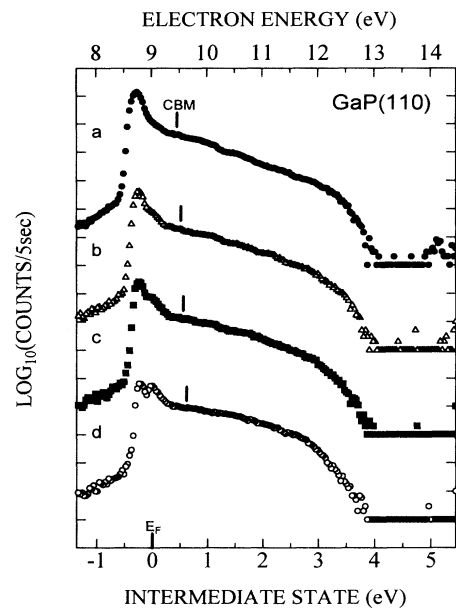


FIG. 5. Photoelectron spectra for surfaces before and after 580-nm dye laser irradiation at  $1.2 \text{ J/cm}^2$ , probed by 3-ps pulses of 4.66 eV light. Dye-laser shot numbers on the surface are as follows: (a) an  $\text{Ar}^+$ -sputtered surface before laser irradiation; irradiated after (b) 20 shots; (c) 40 shots; and (d) 100 shots. The energy scale at the top is measured electron kinetic energy, including the  $-8.88\text{-V}$  sample bias. The energy scale at the bottom is the two-photon intermediate state relative to the Fermi level at the surface. Electron counts per 5-s interval is plotted on a logarithmic scale. The 4.66-eV probe laser intensity was approximately  $19 \text{ MW/cm}^2$ .

Fig. 5 is the pulsed-laser enhancement of the yield around 1.5 eV in the intermediate state spectrum, similar to that observed for  $1 \times 1$  ordered surfaces. The straight shape in the energy distribution curve above 0.4 eV intermediate state on the  $\text{Ar}^+$ -sputtered surface changed to the round shape as laser irradiation was accumulated. The position of the Fermi level ( $E_i=0$ ) relative to the CBM changed from  $-0.45$  eV in (a) to  $-0.62$  eV in (d). The latter is very close to the location of  $E_F$  (0.63 eV below CBM) on the  $1 \times 1$  ordered surface shown in Fig. 1. Apparently the energy distribution curve which is taken at a laser-damaged spot is becoming similar to one taken at a thermally annealed surface.

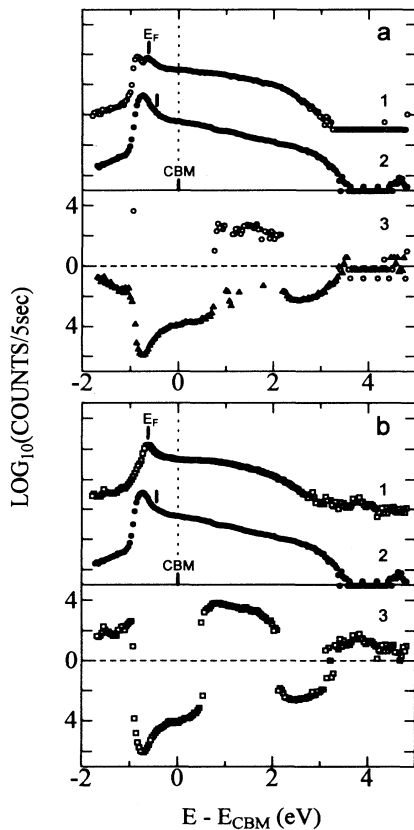


FIG. 6. Energy distribution spectra for (a) the  $\text{Ar}^+$ -sputtered surfaces before pulsed dye-laser irradiation [identical to Fig. 5(a), denoted as curve 2] and after it [identical to Fig. 5(d), denoted as curve 1], as well as a subtracted spectrum (denoted as curve 3) of curve 2 from curve 1; and for (b) the  $\text{Ar}^+$ -sputtered surfaces before thermal annealing [identical to Fig. 5(a), curve 2] and after it (identical to Fig. 1, curve 1) as well as a subtracted spectrum (curve 3). The intermediate-state energy is measured relative to the conduction-band minimum (see text). In curve 3, the magnitudes of the positive and negative subtracted yield are plotted above and below the broken line on positive logarithmic scales, respectively.

Even though the laser irradiation above  $F_D$  causes growth of defects, believed to include vacancy clusters whose boundaries become step edges, other sputter-induced defects may be eliminated from larger areas of the sample not adjacent to vacancy cluster boundaries. To illustrate the similarity of changes in the  $\text{Ar}^+$ -disordered surface produced by pulsed laser exposure (fluence above  $F_D$ ) and by thermal annealing, refer to Fig. 6. Figure 6(a) shows energy distribution spectra for the  $\text{Ar}^+$ -sputtered surfaces before [Fig. 5(a)] and after [Fig. 5(d)] dye-laser irradiation, as well as a subtracted spectrum of Fig. 5(a) from Fig. 5(d). Similarly Fig. 6(b) shows those before [Fig. 5(a)] and after (Fig. 1) thermal annealing including a subtracted spectrum of Fig. 5(a) from Fig. 1. The plots of Fig. 6 are made on a scale of the intermediate energy measured relative to the CBM, because of the different locations of  $E_F$  relative to the band edges on sputtered vs laser irradiated or thermally annealed surfaces, discussed above. The close similarity of the two subtracted spectra suggests that pulsed dye-laser irradiation *below the band gap* of GaP can remove sputter-induced defects, leaving a surface which appears in defect-sensitive photoelectron spectra to be similar to that produced by thermal annealing.

#### IV. CONCLUSION

We measured photoelectron emission from transiently populated states on  $1 \times 1$  ordered,  $\text{Ar}^+$ -sputtered, and pulsed dye-laser irradiated GaP(110) surfaces. A higher density of defect states created in the band-gap region was detected for an  $\text{Ar}^+$ -sputtered surface, compared to that for a  $1 \times 1$  ordered surface. A reduction of photoelectron yield observable from the hot-electron plateau region was found on the disordered surface, relative to the  $1 \times 1$  ordered surface. Pronounced structure originating from the intrinsic surface state on  $1 \times 1$  GaP(110) was not detected. Instead, the gap states are attributed to defects, such as adatoms and bulk disorder on  $\text{Ar}^+$ -sputtered samples, and step edges or Ga droplets on both thermally annealed samples and those exposed to subband-gap pulsed laser. Picosecond-time-resolved measurements of the lifetime of transiently excited states in the band-gap and conduction-band regions on these two surfaces show that the photopopulated defect states relax in less than the 3-ps experimental resolution, regardless of intermediate-state energy in the range 0.17–0.94 eV above  $E_F$ .

#### ACKNOWLEDGMENTS

This work was supported partly by the International Collaboration Program of the Japan Society for Promotion of Science and partly by NSF Grants Nos. DMR-9206745 and DMR-9510297. We are thankful to Professor N. Itoh and Professor Y. Nakai for helpful suggestions.

- <sup>1</sup> J. M. Liu, Y. H. Kurz, and N. Bloembergen, *Appl. Phys. Lett.* **39**, 755 (1981).
- <sup>2</sup> M. Ichige, Y. Matsumoto, and A. Namiki, *Nucl. Instrum. Methods Phys. Res. Sect. B* **33**, 820 (1988).
- <sup>3</sup> P. D. Brewer, J. J. Zinck, and G. L. Olson, in *Laser Ablation*, edited by J. C. Miller and R. F. Haglund, Jr. (Springer, Berlin, 1991), p. 96.
- <sup>4</sup> R. W. Dreyfus, R. Kelly, and R. E. Walkup, *Appl. Phys. Lett.* **49**, 1478 (1986).
- <sup>5</sup> A. Okano, J. Kanasaki, Y. Nakai, and N. Itoh, *J. Phys. Condens. Matter* **6**, 2697 (1994).
- <sup>6</sup> Y. Kumazaki, Y. Nakai, and N. Itoh, *Phys. Rev. Lett.* **59**, 2883 (1987).
- <sup>7</sup> S. S. Goldberg, J. P. Long, and M. N. Kabler, in *Surface Chemistry and Beam-Solid Interactions*, edited by H. Atwater, F. A. Houle, and D. Lowndes, *MRS Symposia Proceedings No. 201* (Materials Research Society, Pittsburgh, 1991), p. 519.
- <sup>8</sup> J. P. Long, S. S. Goldberg, and M. N. Kabler, *Phys. Rev. Lett.* **68**, 1014 (1992).
- <sup>9</sup> N. Itoh, A. Okano, J. Kanasaki, and Y. Nakai, *Ann. Rev. Mater. Sci.* **25**, 97 (1994).
- <sup>10</sup> L. Dirnberger, P. E. Dyer, S. Farrar, P. H. Key, and P. Monk, *Appl. Surf. Sci.* **69**, 216 (1993).
- <sup>11</sup> R. L. Webb, L. C. Jensen, S. C. Landford, and J. T. Dickinson, *J. Appl. Phys.* **74**, 2323 (1993).
- <sup>12</sup> R. W. Dreyfus, F. A. McDonald, and R. J. von Gutfeld, *J. Vac. Sci. Technol. B* **5**, 1521 (1987).
- <sup>13</sup> K. Hattori, A. Okano, Y. Nakai, N. Itoh, and R. F. Haglund, Jr., *J. Phys. Condens. Matter* **3**, 7001 (1991).
- <sup>14</sup> K. Hattori, A. Okano, Y. Nakai, and N. Itoh, *Phys. Rev. B* **45**, 8424 (1992).
- <sup>15</sup> J. Kanasaki, A. Okano, K. Ishikawa, Y. Nakai, and N. Itoh, *J. Phys. Condens. Matter* **5**, 6497 (1993).
- <sup>16</sup> A. Okano, J. Kanasaki, Y. Nakai, and N. Itoh (unpublished).
- <sup>17</sup> M. W. Rowe, H. Liu, G. P. Williams, Jr., and R. T. Williams, *Phys. Rev. B* **47**, 2048 (1993).
- <sup>18</sup> J. Boker, R. Storz, R. R. Freeman, and P. H. Bucksbaum, *Phys. Rev. Lett.* **57**, 881 (1986).
- <sup>19</sup> R. Haight and J. Bokor, *Phys. Rev. Lett.* **56**, 2846 (1986).
- <sup>20</sup> R. Haight and J. A. Silberman, *Phys. Rev. Lett.* **62**, 1815 (1989).
- <sup>21</sup> R. Haight, J. Bokor, J. Stark, H. Storz, R. R. Freeman, and P. H. Bucksbaum, *Phys. Rev. Lett.* **54**, 1302 (1985).
- <sup>22</sup> A. Okano, K. Hattori, Y. Nakai, and N. Itoh, *Surf. Sci.* **258**, L671 (1991).
- <sup>23</sup> A. Huijser, J. Van Laar, and T. L. Van Rooy, *Surf. Sci.* **62**, 472 (1977).
- <sup>24</sup> G. M. Guichard, C. A. Sebenne, and C. D. Thuault, *J. Vac. Sci. Technol.* **16**, 1212 (1979); *Surf. Sci.* **86**, 789 (1978).
- <sup>25</sup> D. Straub, V. Dose, and W. Altmann, *Surf. Sci.* **133**, 9 (1983).
- <sup>26</sup> D. W. Niles and H. Hochst, *Phys. Rev. B* **39**, 7769 (1989).
- <sup>27</sup> M. Yamada, J. Kanasaki, N. Itoh, and R. T. Williams (unpublished).
- <sup>28</sup> C. S. Wang and B. M. Klein, *Phys. Rev. B* **24**, 3393 (1981).
- <sup>29</sup> P. Chiaradia, M. Fanfoni, P. Nataletti, P. De Padova, L. J. Brillson, M. L. Slade, R. E. Viturro, D. Kilday, and G. Margaritondo, *Phys. Rev. B* **39**, 5128 (1989).
- <sup>30</sup> F. J. Himpsel, *Surf. Sci. Rep.* **12**, 1 (1990).
- <sup>31</sup> D. Straub, M. Skibowski, and F. J. Himpsel, *J. Vac. Sci. Technol. A* **3**, 1484 (1985).
- <sup>32</sup> T. Riesterer, P. Perfetti, M. Tschudy, and B. Reihl, *Surf. Sci.* **189/190**, 795 (1987).
- <sup>33</sup> D. Straub, M. Skibowski, and F. J. Himpsel, *Phys. Rev. B* **32**, 5237 (1985).
- <sup>34</sup> Zuejun Zue, S. B. Zhang, S. G. Louie, and M. L. Cohen, *Phys. Rev. Lett.* **63**, 2112 (1989).
- <sup>35</sup> W. Drube, D. Straub, and F. J. Himpsel, *Phys. Rev. B* **35**, 5563 (1987).
- <sup>36</sup> C. Mailhot, C. B. Duke, and D. J. Chadi, *Phys. Rev. B* **31**, 2213 (1984).
- <sup>37</sup> G. P. Srivastava and R. P. Martin, *J. Phys. Condens. Matter* **4**, 2009 (1991).
- <sup>38</sup> M. Gajdardziska-Josifovska, M. R. McCartney, and D. J. Smith, *Surf. Sci.* **287**, 1062 (1993).
- <sup>39</sup> A. Okano, A. Y. Matsuura, K. Hattori, N. Itoh, and J. Singh, *J. Appl. Phys.* **73**, 3158 (1993).